Optical conductivity of high-T_c cuprate thin films deposited by multi-target laser ablation

2000 J. Phys.: Condens. Matter 12 1517

(http://iopscience.iop.org/0953-8984/12/7/332)

J. Phys.: Condens. Matter **12** (2000) 1517–1525. Printed in the UK PII: S0953-8984(00)04355-1

Optical conductivity of high-T_c cuprate thin films deposited by multi-target laser ablation

Sandrine Pessaud†, François Gervais†, Domingos de Sousa‡, Ricardo Lobo§, Corinne Champeaux‖, Pascal Marchet‖, Alain Catherinot‖, Jean Louis Longuet¶ and Frédéric Ravel¶

† Laboratory of Electrodynamics of Advanced Materials, associated with Commissariat à l'Énergie Atomique (CEA) LRC M01, Faculty of Sciences and Techniques, François Rabelais University, 37200 Tours, France
‡ Centre de Recherches sur les Matériaux à Haute Température—CRNS, 45071 Orléans Cédex 2, France
§ Laboratoire de Physique des Solides de l'École Normale Supérieure, Paris, France
‖ Science des Procédés Cérmiques et de Traitements de Surface, UMR CNRS 6638, Faculté des Sciences, Université de Limoges, 87060 Limoges, France
¶ Commissariat à l'Énergie Atomique (CEA), Centre du Ripault, BP 16, 37260 Monts, France

Received 17 May 1999, in final form 6 December 1999

Abstract. Superconducting cuprate thin films were grown upon MgO single crystals by alternating laser pulses in controlled sequences upon an insulating $MCuO_2$ target (M = Ca, Sr) and a $YBa_2Cu_3O_{7-\delta}$ (YBCO) target. The infrared conductivity of the series of films obtained by this multi-target laser ablation technique is deduced from the analysis of infrared reflectivity. The method of fitting by a 'double-damping' Drude model is emphasized and applied to cuprate thin films in a situation in which current Kramers–Kronig analysis is hardly applicable. The agreement of experiment and model is found to be as good as for other conducting oxides investigated previously, including those without transition-metal elements. The concentration dependence of the infrared conductivity profile is discussed.

1. Introduction

Since the discovery of high-temperature oxide superconductors by Bednorz and Müller [1] more than ten years ago, extensive research effort has attempted to raise the critical temperature to extend the field of potential industrial applications. But the critical temperature seems to saturate at the 135 K [2] at ambient pressure in mercury cuprates discovered already six years ago. In the meantime, numerous studies have shown that the electronic properties of high-temperature oxide superconductors are highly 'anomalous' in that they are, even in the normal state, seemingly different from those of conventional metals. The challenge to understand them is probably as important in the normal phase as in the superconducting phase. Inspection of the enormous literature about the subject shows that there is a consensus about the requirement of bidimensionality of cuprates to achieve high-T_c superconductivity [3]. All known 3D cuprates indeed are conductors, but never superconductors [4]. The lack of predictability of existing models and theories about T_c or other superconducting properties encourages us to explore new ways. Since the denominator common to all high-T_c cuprates is bidimensionality (conducting CuO_2 planes alternating with charge reservoir blocks, see a review in [5] for example), epitaxial growth of new cuprate materials appears as a promising method. Among other techniques, laser ablation is known to allow the fabrication of high-quality $YBa_2Cu_3O_{7-\delta}$ (denoted YBCO) films [6]. It is also the major technique to grow infinite-layer compounds [7, 8]. Here we report, for the first time to our knowledge, the results of a systematic study by using two targets in a laser-ablation configuration. By alternating a number m of consecutive laser pulses on a first target of a material A showing a property P_A, then a number n of consecutive pulses on a second target B showing a property P_B, and repeating the sequence, one may build a new material of tentative composition A_m B_n. What will be its properties? P_A, P_B, or something else? In general, we must confess that, in the present state of knowledge, we have no predictability about the tentative property of the film. In addition, if the conditions of depositions are optimized for target A, the actual composition of the deposited film may deviate from A_mB_n. In this paper, we report the preliminary result of a study where A is chosen to be a well known high-T_c superconductor, YBCO, for which, in addition, optimized deposition conditions by laser ablation are known [6], and B is an insulator material $MCuO_2$ (M = Ca, Sr). The choice was justified by the hope of seeing the bidimensional structure of YBCO help in texturing the species from the $MCuO_2$ target to form additional conducting CuO_2 planes.

The most apparent signature of the behaviour of the charge carriers in cuprates is their essentially non-Drude character in the infrared and visible ranges (see review in [9] for example). Several interpretations of the optical conductivity of cuprates have been proposed: a Drude term with a frequency-dependent effective mass and a frequency-dependent damping [10–12], a Drude term plus mid-infrared bands due to polarons [13–16], or due to transitions involving localized states [13], carriers in a Mott insulator [17], theories based on models such as the t–J model in which effects of strong correlations are dominant [18, 19], phenomenological models based on interactions between quasi-particles, the marginal Fermi liquid [20], the nested Fermi liquid [21, 22] or the nearly antiferromagnetic Fermi liquid [23], or even more exotic models [24], and others . . . . No description seems to give rise to a consensus yet. Some of them are specific to cuprates in that they explicitly consider the supposed arrangement of magnetic moments of copper ions and their interactions. Others are based upon more general concepts. But actually, all conducting oxides, not only cuprates or oxides of transition metals but also others, seem to deviate from conventional metal descriptions (see e.g. the review papers [25], [26]). The phenomenon is even more general since other non-metallic materials like conducting polymers also show strong deviations from conventional Drude behaviour [27].

On the other hand, most of the experimental data exploited in the various analyses of cuprates are based upon a Kramers–Kronig (KK) inversion of infrared and visible reflectivity spectra. This method of analysis raises specific problems for spectra which show remaining dispersion outside the spectral range investigated experimentally, which is the case in all conducting materials, at low and high frequency. Of course, one can extrapolate the data down to zero to improve the quality of the KK calculations, but then, one has to make an assumption about the type of chosen profile. By doing so, one should keep in mind that (i) no microscopic model applies successfully in the whole spectral range to our knowledge, (ii) the calculated conductivity is extremely sensitive to the inaccuracy of the low-frequency reflectivity data. One faces, therefore, the need for a model as simple as possible, preferentially showing some continuity with the original Drude concept, but as general as possible and applicable, therefore, to any conducting oxide. The desired model should allow a parametrization of any conductivity spectrum to allow subsequent comparison of the electronic properties of oxides belonging to different families. The purpose of this paper is to show that a ‘double-damping’ Drude model, already found to fit the spectral conductivity of a wide variety of oxides [25, 26, 28–38], applies to cuprate thin films equally well.

There is an additional problem that prevents the more straightforward Kramers–Kronig analysis. The thickness of the films is such that the infrared radiation also experiences the substrates in certain spectral ranges, depending on the chemical composition of the film. The causality relationships at the origin of the Kramers–Kronig analysis assume a continuous medium, not a multi-layer compound as is the case of our samples. Conversely, the dielectric response (or optical conductivity) of the substrate is well known. It is easier, therefore, to reconstruct the optical response of the system by fitting the dielectric response of the upper layer to the total response, which is performed here.

2. Double-damping Drude model

The conventional Drude model is unable to take into account all kinds of excitations which are currently observed in conducting oxides (phonons, plasmons, superconducting condensate, relaxators, polarons, mid-infrared bands . . .) [25, 26, 29–39]. In the presence of oscillators and plasmon in the same frequency range, the following expression (double-damping Drude model [30–32, 37]) has been shown to allow the separate determination of phonons (or oscillators of another type) and plasmon parameters

$$\tilde{\varepsilon} = \varepsilon_\infty \left[\prod_j \frac{\Omega_{jLO}^2 - \omega^2 + \mathrm{i}\gamma_{JLO}\omega}{\Omega_{jTO}^2 - \omega^2 + \mathrm{i}\gamma_{jTO}\omega} - \frac{\Omega_p^2 - \mathrm{i}(\gamma_p - \gamma_0)\omega}{\omega(\omega - \mathrm{i}\gamma_0)} \right]. \quad (1)$$

The first term of the right-hand side is aimed to describe excitations with a restoring force constant (like phonons or trapped polarons), whereas the second term discriminates those without restoring force constant (like charge carriers, polarons above the mobility edge, superconducting condensate). The model is straightforwardly deduced from the Kurosawa [40] relation that is itself an extension of the Lyddane–Sachs–Teller relationship. The general context of such an approach is nothing but the Maxwell equations which state that transverse optical (TO) modes are the complex poles of the dielectric function $\tilde{\varepsilon}$, while longitudinal optical modes satisfy $\tilde{\varepsilon} = 0$, hence are the complex zeros of $\tilde{\varepsilon}$. Ω stands for frequencies and γ for dampings. Note that, in the absence of phonons or other oscillators, the above formula reduces to the simple Drude expression when $\gamma_p = \gamma_0$. Here γ_p represents the linewidth of the plasma response centred at $\omega = \Omega_p$. γ_0 is the linewidth of absorption centred at $\omega = 0$.

One feature common to conducting oxides is a plasma edge which is highly shifted down (in the infrared) with respect to that of normal metals. This is related to the lower electronic concentration n and/or high electron effective mass $m*$

$$\Omega_p^2 = \frac{ne^2}{\varepsilon_v \varepsilon_\infty m^*}. \quad (2)$$

Moreover the plasma response is highly damped, even overdamped, in most cases. The ratio γ_p/Ω_p is an indication about the type of motion of charge carriers, normally vibrational when the ratio is small, diffusive or incoherent, phenomenologically relaxational, when the ratio is large.

3. Multi-target laser-ablated thin films

The compositions of the series Y_3C_n (Y_3 for three pulses on YBCO, C_n for n pulses on $CaCuO_2$), measured by Castaing microprobe [41] are given in table 1. Since the thickness of the films was of the order of 200 nm, the charge carrier concentration is not sufficient to absorb infrared radiation completely. A part of the radiation is reflected at the film–MgO

Table 1. Critical temperatures and composition of the series Y_3C_n measured by Castaing microprobe written in several forms. One of the forms (second column) assumes that the YBCO skeleton is kept upon adding a random CaO sheet in the reservoir block.

Films	Chemical composition	Chemical composition	Chemical composition	T_{onset} (K)	$T_{R=0}$ (K)
Y_3C_3	$YBa_2Ca_{3.1}Cu_{5.6}O_{12.2}$	$(Y_{0.54}Ca_{0.46})(Ba_{0.54}Ca_{0.46})_2Ca_{0.28}Cu_3O_{6.55}$		74	52
Y_3C_4	$YBa_2Ca_{4.1}Cu_{6.6}O_{14.2}$	$(Y_{0.45}Ca_{0.55})(Ba_{0.45}Ca_{0.55})_2Ca_{0.21}Cu_3O_{6.44}$		65	49
Y_3C_5	$YBa_2Ca_5Cu_{7.6}O_{16.1}$	$(Y_{0.40}Ca_{0.60})(Ba_{0.40}Ca_{0.60})_2Ca_{0.14}Cu_3O_{6.34}$	$YBa_2Cu_3O_7 + \approx 5\ CaCuO_2$	72	55
Y_3C_6	$YBa_2Ca_{5.9}Cu_{8.5}O_{17.9}$	$(Y_{0.35}Ca_{0.65})(Ba_{0.35}Ca_{0.65})_2Ca_{0.13}Cu_3O_{6.24}$	$YBa_2Cu_3O_7 + \approx 5.5\ CaCuO_2$	65	<25
Y_3C_7	$YBa_2Ca_6Cu_{9.7}O_{20.2}$		$YBa_2Cu_3O_7 + \approx 6\ CaCuO_2$	67	50
Y_3C_9	$YBa_2Ca_{8.9}Cu_{11.4}O_{23.8}$		$YBa_2Cu_3O_7 + \approx 8.5\ CaCuO_2$		
Y_3C_{12}	$YBa_2Ca_{12.3}Cu_{15.3}O_{31.1}$		$YBa_2Cu_3O_7 + \approx 12.3\ CaCuO_2$		

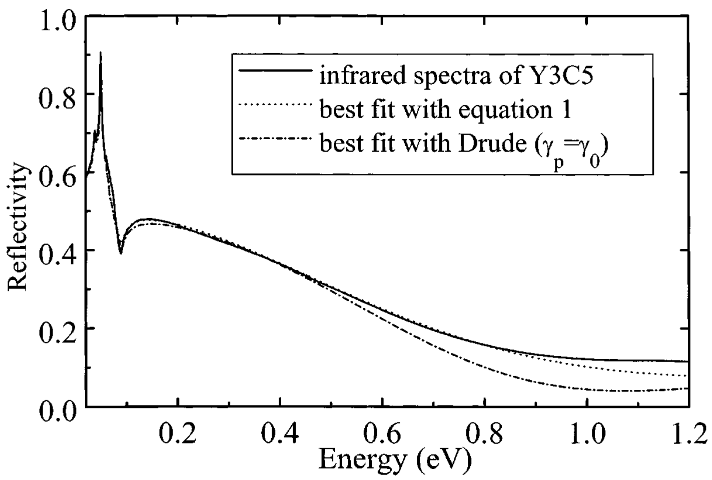

Figure 1. Comparison of best fits of the extended Drude model (dotted line) and the conventional Drude model (chain line) to the reflectivity spectrum of the film Y_3C_5 (solid line).

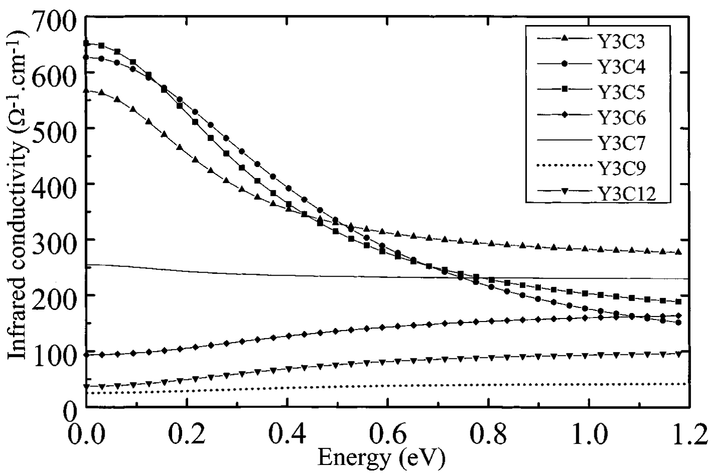

Figure 2. Sequence of infrared conductivity profiles of Y_3C_n films.

interface, yielding a signature in all spectra. We take account of this contribution in the fitting procedure. On the other hand, the charge carrier concentration is high enough in all films to screen the phonons, largely or almost completely. By comparison with the spectra of cuprate single crystal samples [9, 26, 32, 36, 40] for the polarization parallel to the *c* axis which shows the sole response to unscreened phonons, epitaxy of the films is most likely achieved. Phonons indeed are highly screened in films that display superconductivity. An example of best fit of the model to the reflectivity data is shown in figure 1. Repeating the procedure for all films yields the composition dependence of the optical conductivity (restricted to charge carriers, phonon contribution withdrawn) shown in figure 2. The low-frequency conductivity compares well with measured DC values as shown in table 2 (agreement within 20% on average).

Since the films have not been treated to optimize doping after the growth, roughly speaking the number of charge carriers is related to the relative number of species from the YBCO target. It is seen in figure 2 that the surface under the optical conductivity

Table 2. Comparison between far-infrared and DC conductivities of different films.

Films	Infrared conductivity (Ω^{-1} cm^{-1})	DC conductivity (Ω^{-1} cm^{-1})
$Y_{24}S_8$	2620	3595
$Y_{24}S_{12}$	2220	2340
$Y_{24}S_{18}$	1290	1500
$Y_{24}S_{124}$	675	580
$Y_{24}S_{30}$	400	484
$Y_{24}C_6$	1950	2350
$Y_{24}C_{12}$	1180	1530
$Y_{24}C_{18}$	900	1170
$Y_{24}C_{24}$	380	373
$Y_{24}C_{30}$	315	420
$Y_{12}C_{12}$	525	671
$Y_{12}C_{18}$	340	430
$Y_{12}C_{24}$	100	120
$Y_{12}C_{30}$	225	160
Y_3C_3	554	727
Y_3C_4	640	464
Y_3C_5	660	419
Y_3C_7	250	220

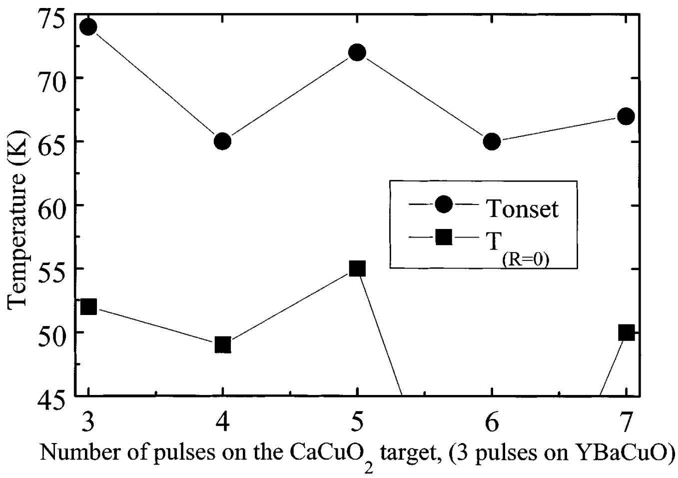

Figure 3. Composition dependence of superconducting properties of Y_3C_n films.

(integrated intensity $\int \sigma(\omega)\,d\omega = (\pi e^2/2)n/m^*$ indeed roughly follows the percentage of YBCO ablated to build each film. The profiles of optical conductivity also appear roughly related to the integrated intensity. For highest carrier densities (Y_3C_3 to Y_3C_5 films), a broad Drude peak is observed in the low-frequency conductivity. Conversely, for the sample Y_3C_7, although the sample is still a superconductor, the optical conductivity is almost flat. For other samples, the optical conductivity decreases upon lowering frequency, what is the reverse of conventional Drude model expectations. The samples are superconductors up to $n/m = 7/3$ (figure 3). It should be emphasized that figure 2 displays a beautiful sequence of conductivity profiles evolving from near-Drude-like at highest carrier concentration, to flat and to 'inverse-Drude-like' in that the conductivity is the lowest at low frequency.

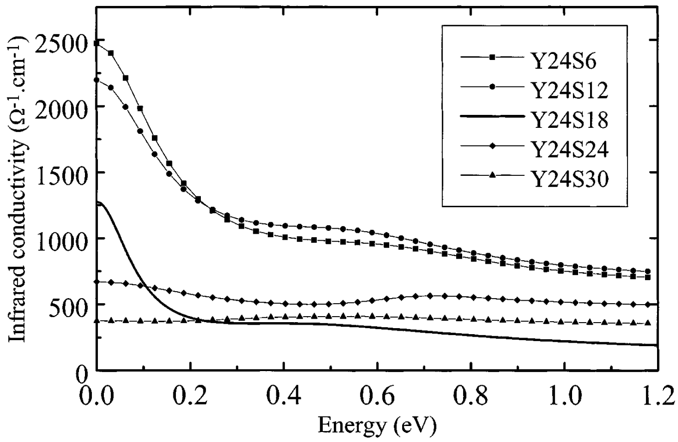

Figure 4. Sequence of infrared conductivity profiles of $Y_{24}S_n$ films.

The extrapolation of this tendency consistently suggests the onset of a low-frequency gap for insulating samples. The low-carrier-concentration profiles display a broad bump in the mid-infrared. The signature of possible trapped polarons is just expected in this spectral range [15]. This sequence of conductivity profiles versus concentration suggests, therefore, several regimes of conductivity.

- For low-carrier concentration, the infrared conductivity is consistent with trapped polarons plus a relatively small number of large polarons above the mobility edge. Examples are Y_3C_9 and Y_3C_{12}. These samples do not show superconductivity.
- For higher carrier concentration, the conductivity profile appears almost flat over a wide spectral range, suggesting incoherent carrier transport. Trapped polarons still are supposed to contribute to the conductivity.
- For largest carrier concentrations, the conductivity becomes more and more Drude-like even if the actual mechanism appears actually more complex than suggested by the conventional Drude model.

We conjecture here the relevance of the polaronic model because the phonons are screened, but *never completely screened* in any of our films, indicating that the Coulombic field is still partly efficient. In these conditions, charge carriers necessarily interact with ions. The polaron concept applies therefore.

The mid-infrared trapped-polaron band is even more pronounced in the series $Y_{24}S_n$ (figure 4), where S stands for the insulating target $SrCuO_2$. For all the samples of this series, an additional broad oscillator in the region 0.5–0.7 eV was required. All samples were found to be superconductors. Again, depending on the amount of species from the YBCO target which ensures doping, the conductivity profile evolves from Drude-like for low n/m ratios to flat for high n/m ratios.

4. Summary

The 'double-damping' Drude model has been shown to fit the infrared and optical reflectivity of high-T_c superconducting films deposited by the original multi-target laser ablation technique very closely, even though some of the spectra extend over more than three orders of magnitude in energy. The more common Kramers–Kronig procedure would not be straightforwardly applicable in this multi-layer system. The conductivity spectra have been parametrized with a very restricted number of parameters for subsequent comparison with other conducting oxides. The occurrence of a polaron contribution is suggested. Polarons appear to be trapped at energies around 0.5 eV for low x (or low YBCO percentage ablated), soften with increasing doping and then tend to merge in the pseudo-Drude response for largest doping.

References

[1] Bednorz J G and Müller K A 1986 *Z. Phys.* B **64** 189

[2] Putilin S N, Antipov E V, Chmaissem O and Marezio M 1993 *Nature* **362** 226

[3] Ginsberg D M (ed) 1992 *Physical Properties of High Temperature Superconductors III* (Singapore: World Scientific)

[4] Webb A W, Skelton E F, Quadri S B, Browning V and Carpenter E R Jr 1992 *Phys. Rev.* B **45** 2480

[5] Raveau B, Michel C, Herieu M and Groult D 1991 *Crystal Chemistry of High-T_c Superconducting Oxides* (New York: Springer)

[6] Marchet P, Champeaux C, Mercurio J P and Catherinot A 1993 *J. Physique III* **3** 767
Champeaux C, Damiani D, Aubreton J and Catherinot A 1993 *Appl. Surf. Sci.* **69** 169
Champeaux C, Marchet P, Aubreton J, Mercurio J P and Catherinot A 1993 *Appl. Surf. Sci.* **69** 335

[7] Norton D O, Chakoumakos B C, Budai J D and Lowdes D H 1993 *Appl Phys. Lett.* **62** 1679
Balesstrino G, Desfeux R, Matellucci S, Paoletti A, Petrocelli G, Tebano A, Mercey B and Hervieu M 1995 *J. Mater. Chem.* **5** 1879–1883
Tsukamoto A, Wen J G, Nakanishi K and Tanabe K 1997 *Physica C* **292** 17

[8] Hiroi Z, Azuma M, Takano M and Takeda Y 1993 *Physica C* **208** 286
Zhang H, Wang Y Y, Dravid V P, Marks L D, Han P D, Payne D A, Radaelli P G and Jorgensen J D 1994 *Nature* **370** 352

[9] Tanner D B and Timusk T 1992 *Physical Properties of High Temperature Superconductors III* ed D M Ginsberg (World Scientific) pp 363–469

[10] Schlesinger Z, Collins R T, Holtzberg F, Field C, Koren G and Gupta A 1990 *Phys. Rev.* B **41** 11 237

[11] El Azrak A, Nahoon R, Boccara A C, Bontemps N, Guilloux-Viry M, Thiret C, Perrin A, Li Z Z and Raffy H 1993 *J. Alloys Compounds* **195** 663

[12] Romero C D, Porter D B and Tanner 1992 *Solid State Commun.* **82** 183

[13] Mikhailovic D, Foster C M, Voss K and Hegeer A J 1990 *Phys. Rev.* B **42** 7889

[14] Emin D 1993 *Phys. Rev.* B **48** 139 961

[15] Eagles D, Lobo R P S M and Gervaus F 1995 *Phys. Rev.* B **52** 6440

[16] Calvani P, Capizzi M, Lupi S, Maselli P and Paolone A 1996 *Phys. Rev.* B **53** 2756

[17] Rice T M and Zhang F C 1989 *Phys. Rev.* B **39** 815

[18] Lorenzana J and Yu L 1993 *Phys. Rev. Lett.* **70** 861

[19] Riera J A and Dagotto E 1994 *Phys. Rev.* B **50** 452

[20] Varma C M, Littlewood P B, Schmitt-Rink S, Abrahams E and Ruckenstein A E 1989 *Phys. Rev.* B **63** 1996

[21] Littlewood P B and Varma C M 1991 *J. Appl. Phys.* **69** 4979

[22] Ruvalds J and Virosztek A 1991 *Phys. Rev.* B **43** 5498

[23] Monthoux P and Pines D 1993 *Phys. Rev.* B **47** 6069

[24] Anderson P W 1997 *Phys. Rev.* B **55** 11 785

[25] Gervais F, Lobo R P S M, Licheron M and Gotor F J 1996 *Ferroelectrics* **177** 107

[26] Gervais F and Lobo R P S M 1997 *Z. Phys.* B **104** 681

[27] Petit N, Gervais F, Buvat P, Hourquebie P and Topart P *Eur. Phys. J.* B at press

[28] Bassat J M, Odier P and Gervais F 1987 *Phys. Rev.* B **35** 7126

[29] Baumard J F and Gervais F 1977 *Phys. Rev.* B **15** 2316

[30] Gervais F 1981 *Phys. Rev.* B **23** 6580

[31] Gervais F 1983 *Infrared and Millimeter Waves* vol 8, ed K J Button (New York: Academic) pp 279–339

[32] Gervais F, Echegut P, Bassat J M and Odier P 1988 *Phys. Rev.* B **37** 9364

[33] Gervais F, Servoin J L, Baratoff A, Bednorz J G and Binnig G 1993 *Phys. Rev.* B **47** 8187

[34] Lobo P S M, Gervais F, Champeaux C, Marchet P and Catherinot A 1995 *Mater. Sci. Eng.* B **34** 74

[35] Lobo R P S M, Gervais F and Oseroff S B 1997 *Europhys. Lett.* **37** 341

[36] Lobo R P S M, Gotor F J, Odier P and Gervais F 1997 *Phys. Rev.* B **53** 410

[37] Licheron M and Gervais F 1993 *Phys. Rev.* B **47** 8008

[38] Lobo R P S M and Gervais F 1995 *Phys. Rev.* B **52** 13 294

[39] Kurosawa T 1961 *J. Phys. Soc. Japan* **16** 1298
[40] Collins R T, Schlesinger Z, Chandrasshekhr G V and Shafer M W 1988 *Phys. Rev.* B **39** 2251
[41] Pessaud S, Gervais F, Champeaux C, Catherinot A, Licheron M, Longuet J L and Ravel F 1999 *Mater. Sci. Eng.* B **60** 205